Analytical prediction of size-induced ferroelectricity in BaO nanowires under stress

Anna N. Morozovska,[1,*] E. A. Eliseev,[2] Maya D. Glinchuk,[2,†] and Robert Blinc[3]
[1]*V. Lashkarev Institute of Semiconductor Physics, NAS of Ukraine, 41 pr. Nauki, 03028 Kiev, Ukraine*
[2]*Institute for Problems of Materials Science, NAS of Ukraine, Krjijanovskogo 3, 03142 Kiev, Ukraine*
[3]*Jožef Stefan Institute, P.O. Box 3000, 1001 Ljubljana, Slovenia*
(Received 1 November 2009; revised manuscript received 9 January 2010; published 5 March 2010)

We predict that a ferroelectric phase can be induced in otherwise nonferroelectric binary oxides like BaO, EuO and Er_2O_3 by a strong enough stress $\sigma \sim \mu/R$ present under the curved surface in nanowires due to intrinsic surface stress μ. Our analytical calculations performed within the Landau-Ginzburg-Devonshire theory prove that BaO nanowires of radius $R \sim (1-10)$ nm can be ferroelectric at room temperatures with spontaneous polarization values ~ 0.5 C/m^2 for typical surface stress coefficients $\mu \sim (10-50)$ N/m. The same phenomena could lead to high temperature magnetoelectric effect in nanosystems of magnetic binary oxides.

DOI: 10.1103/PhysRevB.81.092101 PACS number(s): 77.80.B−, 68.35.Md

Alkaline and rare earth binary oxides—BaO, MgO, EuO etc.—are of great potential use in microelectronic and nanoelectronic devices.[1–5] The appearance of ferroelectricity and related multifunctional properties seemed however so unlikely that it was never previously experimentally investigated. The binary oxides remained in the complete shadow of multifunctional ABO_3 ferroelectric perovskite oxides.[6–8] Only recently a first-principles density functional calculation showed that strain-induced ferroelectricity may occur in binary oxides and their superlattices under biaxial epitaxial strain.[9] Here we predict that a ferroelectric phase can be induced by strong stress inevitably present under the curved surface due to the positive intrinsic surface stress in nanowires and high aspect ratio cylindrical nanoparticles of otherwise nonferroelectric binary oxides like BaO. In magnetic binary oxides the intrinsic surface stress may thus lead both to induced ferroelectricity and an increase in the ferromagnetic transition temperature in nanorods and nanowires.[10–12]

It should be mentioned that in epitaxial films high misfit strains between the film and the substrate could be relaxed via dislocations[13] that may eliminate the ferroelectric phase. On the other hand the stress that exists under the curved surface in nanowires and nanorods cannot be excluded. The intrinsic surface stress (surface tension) should depend both on the growth conditions and the surface morphology.[14,15] Since the surface tension appears even for the case of nonreconstructed geometrical surface due to the surface break,[15] the surface transformation could in principle affect the surface tension value. Actually, Zang *et al.*[16,17] have found that the surface reconstruction is responsible for the appearance of surface stresses and leads to the self-bending of Si nanofilms. This effect depends on the adsorption characteristics.[17]

Dislocations in ferroelectric nanowires did not appear both in atomistic calculations[18–20] and were not observed experimentally.[21–23] Thus we could ignore dislocations appearance and consider the impact of the intrinsic surface stress of ferroelectric properties only, leaving the problem of the relationship between the surface morphology and stress for further studies.

Here we present the temperature-wire radius phase diagram of BaO nanowires. We as well show the temperature dependence of the spontaneous polarization and its dependence on the wire radius. The calculations were performed within Landau-Ginzburg-Devonshire (LGD) theory.

For nanosized ferroics the applicability of LGD theory is corroborated by the fact, that the critical sizes of the long-range order appearance calculated from atomistic[24] and phenomenological[25,10,11] theories are in good agreement with each other as well as with experimental results for ferromagnetic[26] and ferroelectric[7,21–23,27] systems.

In particular, Yadlovker and Berger[21] reported about the spontaneous polarization enhancement up to $0.25-2$ μC/cm^2 and ferroelectric phase conservation in Rochelle salt nanorods (with diameters about 30 nm and height 500 nm) up to the material decomposition temperature 55 °C that is about 30 °C higher than the one of bulksize crystals. These results were qualitatively explained[10] and quantitatively fitted[11] within LGD theory allowing for the intrinsic surface tension.

Recently LGD predictions[10,11] were corroborated by Cai *et al.*,[19] who used the density functional theory (DFT) to study ferroelectricity and finite-size effects in $PbTiO_3$ nanowires with diameters from 1.4 to 4.2 nm. They have found that the critical radius of ferroelectric phase appearance is about 1.4 nm. Moreover, they have shown that the ferroelectric properties of nanowires are enhanced in comparison with the bulk one due to the intrinsic surface tension.

Geneste *et al.*[18] studied the size dependence of the ferroelectric properties of $BaTiO_3$ nanowires from DFT. They showed that the ferroelectric distortion along the wire axis disappears below a critical size of about 1.2 nm, however it can be recovered under the appropriate strain conditions.

Using DFT, Hong *et al.*[20] showed that polarization distribution over the wire radius is essentially inhomogeneous (different topological configurations are possible), at that the polarization near the surface strongly differs from its average value. Also the critical size of the ferroelectric phase disappearance in $BaTiO_3$ nanowires varies from 2 to 3 unit cells.

Thus, the atomistic calculations of $PbTiO_3$ and $BaTiO_3$ nanowires polar properties[18–20] have shown that the ferroelectric state is stable for wire radiuses 1–10 nm and higher. LGD-type models quantitatively reproduce these results.

The possible atomic structure of the MO wire is shown in Fig. 1. The intrinsic surface stress leads to strains and a cor-

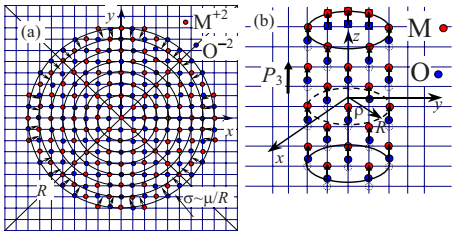

FIG. 1. (Color online) Possible atomic structure of the MO wire: cross-section without dislocations (a) and vertical section (b). Metal M is for Ba, Zn, Mg, Eu, etc.

responding bond length contraction in the radial direction ρ and an elongation along the wire axes z. The stress induces out-of-plane displacements of the light O^{-2} anions, which leads to the unit cell tetragonal distortion and thus can cause a macroscopic dipole moment to appear in the longitudinal direction z (see Fig. 1).

In the phenomenological approach used in this paper, the strains induced by the surface stress lead to the appearance of the spontaneous polarization via electrostriction. Including the surface energy term, the LGD free energy F depends on the component P_3 of the spontaneous polarization and mechanical strains u_{ij} as[9–11,28]

$$F = \left\{ \int_V d^3r \left[\frac{\alpha}{2}P_3^2 + \frac{\beta}{4}P_3^4 + \frac{\gamma}{6}P_3^6 + \frac{g}{2}(\nabla P_3)^2 - P_3\left(E_e + \frac{E_3^d}{2}\right) - q_{ij33}u_{ij}P_3^2 + \frac{c_{ijkl}}{2}u_{ij}u_{kl}\right] + \int_S d^2r\left(\frac{\alpha_S}{2}P_3^2 + \mu_{ij}^S u_{ij}\right)\right\} \quad (1)$$

The surface energy coefficient α_S is positive, isotropic and weekly temperature dependent, so that higher terms can be neglected in the surface energy expansion. The integration is performed over the systems surface S and volume V correspondingly. μ_{ij}^S is the intrinsic surface stress tensor that determines the excess pressure under the curved surface of a solid body.[15] The pressure strongly increases $\sim 1/R$ when the particle radius R decreases. The elastic stiffness tensor is c_{ijkl} and q_{ijkl} stands for electrostriction stress tensor. E_e is the external electric field.

The expansion coefficient γ as well as the gradient term g are positive. The coefficient $\alpha(T)=\alpha_T(T-T_c^*)$ is T dependent, where T is the absolute temperature. T_c^*, which is normally positive for conventional ferroelectrics, here is negative as bulk MO is nonferroelectric. Its value can be determined from the critical strain at zero temperature for thick layers with a flat surface.

For long cylindrical nanoparticles with the spontaneous polarization directed along the cylinder axes the depolarization field E_d can be neglected. At the same time a strong depolarization field exists in spherical nanoparticles.[10,11]

For cubic symmetry nonzero components of the strain tensor inside the cylindrical wire of radius R have the following form:[11] radial strain $u_{\rho\rho}=u_{11}=u_{22}=-(s_{11}+s_{12})(\mu/R)+Q_{12}P_3^2$ and longitudinal strain $u_{33}=-s_{12}(\mu/R)+Q_{11}P_3^2$, where Q_{ij} are the components of electrostriction strain tensor, s_{ij} are the elastic compliances, and in the isotropic approximation $\mu_{ij}^S=\delta_{ij}\mu$. Note that the radial strain $u_{\rho\rho}$ is negative, while the longitudinal strain u_{33} is positive at $P_3=0$, since $(s_{11}+s_{12})>0$ and $s_{12}<0$ for the considered cubic symmetry. Thus the strains induce a bond lengths contraction in radial directions $\{x,y\}$ and an elongation in the z direction. The corresponding tetragonality of the unit cell acquires the form

$$\frac{c}{a} = \frac{1+u_{33}}{1+u_{22}} = \frac{1-s_{12}(\mu/R)+Q_{11}\bar{P}^2}{1-(s_{11}+s_{12})(\mu/R)+Q_{12}\bar{P}^2} \approx 1 + s_{11}\frac{\mu}{R} + (Q_{11}-Q_{12})\bar{P}^2. \quad (2)$$

Using the expressions for strains and the direct variational method, the transition temperature into the ferroelectric phase and the spontaneous polarization $\bar{P}_3(R)$ averaged over the wire radius R can be derived similarly to[10,11] as

$$T_{cr}(R) \approx T_c^* - Q_{12}\frac{4\mu}{\alpha_T R} - \frac{2}{\alpha_T R}\left(\frac{g\alpha_S}{g+2\alpha_S R/k_0^2}\right), \quad (3)$$

$$\bar{P}_3(R) \approx \sqrt{\frac{2\alpha_T(T_{cr}(R)-T)}{\beta+\sqrt{\beta^2+4\gamma\alpha_T(T_{cr}(R)-T)}}}. \quad (4)$$

The constant $k_0=2.408\ldots$ is the minimal root of the Bessel function $J_0(k)$.

The first term in Eq. (3) is negative and size-independent for nonferroelectric oxide layers with a flat surface. The second one is the contribution of the stress $\sigma\sim\mu/R$, whereas the third negative term originates from correlation effects. The third term decreases the possible transition temperature T_{cr} at positive α_S, while the second term increases T_{cr} under the condition $Q_{12}\mu<0$. By changing the wire radius one can tune the transition temperature and polarization value in a wide range.

LGD free energy expansion coefficients for BaO bulk material were extracted from the results of the first principle calculation[9] and experimental data[29] as described in Appendix of Ref. 30. All parameters are listed in the Table I.

TABLE I. LGD free energy expansion coefficients for BaO bulk material.

α_T [m/(FK)]	β [$m^5/(C^2F)$]	γ [$m^9/(C^4F)$]	T_c^* (K)	Q_{11} (m^4/C^2)	Q_{12} (m^4/C^2)	s_{11} (m^2/N)	s_{12} (m^2/N)
6.4×10^6	1.0×10^9	4.4×10^{11}	−226	0.50 ± 0.05	-0.22 ± 0.3	10.23×10^{-12}	-2.91×10^{-12}

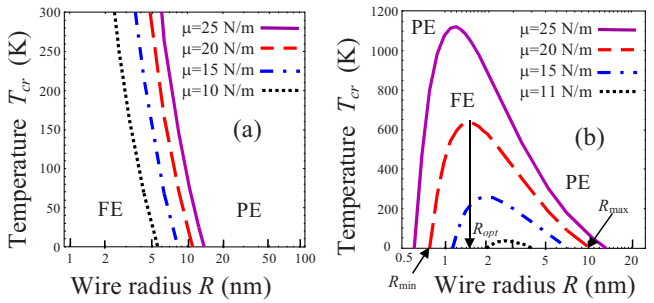

FIG. 2. (Color online) Phase diagrams of BaO nanowires in coordinates temperature-radius for $|\alpha_S| \ll 2\mu|Q_{12}|$ (a) and for $|\alpha_S| \gg 2\mu|Q_{12}|$ (b).

In analogy to perovskites Q_{12} is negative. The surface curvature can thus induce ferroelectricity in BaO nanowires. The phase diagrams of BaO wires in the temperature-wire-radius plane are shown in Figs. 2. The dependence of the spontaneous polarization of BaO nanowires on temperature and radius are shown in Figs. 3. The figures were calculated from Eqs. (2)–(4), with the parameters from Table I and the gradient coefficient $g=2\times10^{-9}$ m^3/F. The surface stress coefficient μ varies in the typical range of 5–50 N/m depending on the nanowire ambient (template material, gel or gas).

The two limiting cases $|\alpha_S| \ll 2\mu|Q_{12}|$ and $|\alpha_S| \gg 2\mu|Q_{12}|$ correspond to large and small contribution of the intrinsic surface stress. It is seen from the Figs. 2 and 3 that BaO nanowires of radius $\sim(1-10)$ nm can be ferroelectric at room and even at higher temperatures (with spontaneous polarization values up to 0.5 C/m^2) for surface stress coefficient $\mu\sim(10-50)$ N/m. The spontaneous polarization increases with the increase of the surface tension coefficient.

Let us underline that the dependence of the transition temperature T_{cr} on the wire radius R is monotonic for the case $|\alpha_S| \ll 2\mu|Q_{12}|$: T_{cr} decreases with increasing wire radius R (Figs. 2(a)). Actually, for the case $T_{cr}(R) \approx T_c^* - Q_{12}\frac{4\mu}{\alpha_T R}$ the critical radius for the appearance the ferroelectricity is $R_{cr}(T) \approx \frac{4\mu Q_{12}}{\alpha_T(T_c^*-T)}$ at a given temperature T. For this limiting case the influence of the correlation effects are negligibly small in comparison with the surface stress contribution. The spontaneous polarization in this case monotonically decreases with the increase of the wire radius and disappears at $R=R_{cr}(0)$ [see Fig. 3(b)].

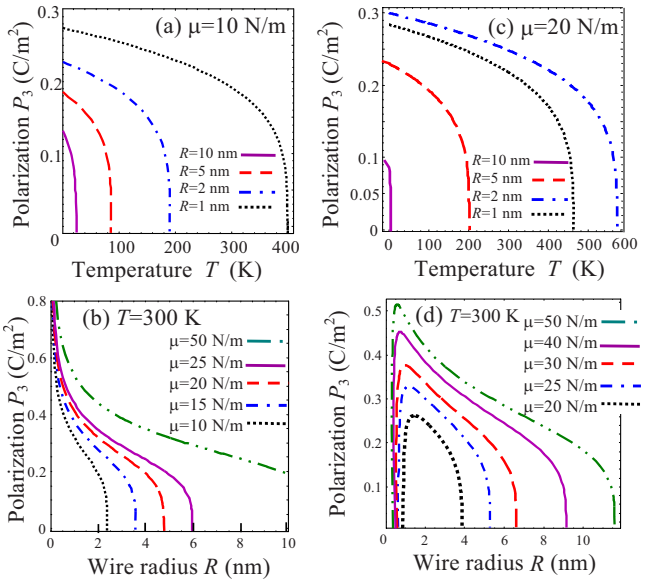

FIG. 3. (Color online) Spontaneous polarization of BaO nanowires vs temperature (a,c) and radius at $T=300$ K (b,d). Plots (a,b) correspond to $|\alpha_S| \ll 2\mu|Q_{12}|$, plots (c,d) correspond to $|\alpha_S| \gg 2\mu|Q_{12}|$.

In the other limiting case $|\alpha_S| \gg 2\mu|Q_{12}|$ the region of the appearance of ferroelectricity is smaller [compare Figs. 2(a) and 2(b)]. Here the dependence of the transition temperature T_{cr} on the wire radius R is not monotonic [see Fig. 3(d)].

To summarize we predict that a ferroelectric phase can be induced in otherwise nonferroelectric binary oxides (BaO, EuO, MgO, Er_2O_3, etc.) by a strong enough stress inevitably present under the curved surface in the high aspect ratio cylindrical nanoparticles and nanowires. Analytical calculations performed within the LGD theory prove that BaO nanowires of radius $\sim(1-10)$ nm can be ferroelectric at room temperatures with spontaneous polarization values ~0.5 C/m^2 for typical surface stress coefficients $\sim(10-50)$ N/m. This could lead to elaboration of high temperature magnetoelectric nanodevices based on magnetic binary oxides. Actually, recent experimental results show that Er_2O_3 nanoparticles of 5–6 nm sizes are indeed ferroelectric and magnetoelectric.[31]

*Corresponding author; morozo@i.com.ua
†Corresponding author; glin@imps.kiev.ua

[1] M. Posternak, A. Baldereschi, H. Krakauer, and R. Resta, Phys. Rev. B **55**, R15983 (1997).
[2] B. B. Karki, R. M. Wentzcovitch, S. de Gironcoli, and S. Baroni, Science **286**, 1705 (1999).
[3] R. A. McKee, F. J. Walker, and M. F. Chisholm, Science **293**, 468 (2001).
[4] C. J. Först, C. R. Ashman, K. Schwarz, and P. E. Blöchl, Nature (London) **427**, 53 (2004).
[5] J. F. Scott, Nature Mater. **6**, 256 (2007).
[6] M. Fiebig, J. Phys. D: Appl. Phys. **38**, R123 (2005).
[7] D. D. Fong, G. B. Stephenson, S. K. Streiffer, J. A. Eastman, O. Auciello, P. H. Fuoss, and C. Thompson, Science **304**, 1650 (2004).
[8] D. D. Fong, A. M. Kolpak, J. A. Eastman, S. K. Streiffer, P. H. Fuoss, G. B. Stephenson, C. Thompson, D. M. Kim, K. J. Choi, C. B. Eom, I. Grinberg, and A. M. Rappe, Phys. Rev. Lett. **96**, 127601 (2006).
[9] E. Bousquet, N. Spaldin, and Ph. Ghosez, Phys. Rev. Lett. **104**, 037601 (2010).
[10] A. N. Morozovska, E. A. Eliseev, and M. D. Glinchuk, Phys. Rev. B **73**, 214106 (2006).
[11] A. N. Morozovska, M. D. Glinchuk, and E. A. Eliseev, Phys.

Rev. B **76**, 014102 (2007).
[12] M. D. Glinchuk, E. A. Eliseev, A. N. Morozovska, and R. Blinc, Phys. Rev. B **77**, 024106 (2008).
[13] J. S. Speck and W. Pompe, J. Appl. Phys. **76**, 466 (1994).
[14] F. Liu and M. G. Lagally, Phys. Rev. Lett. **76**, 3156 (1996).
[15] V. A. Shchukin and D. Bimberg, Rev. Mod. Phys. **71**, 1125 (1999).
[16] J. Zang, M. Huang, and F. Liu, Phys. Rev. Lett. **98**, 146102 (2007).
[17] J. Zang and F. Liu, Nanotechnology **18**, 405501 (2007).
[18] G. Geneste, E. Bousquest, J. Junquera, and P. Ghosez, Appl. Phys. Lett. **88**, 112906 (2006).
[19] M. Q. Cai, Y. Zheng, B. Wang, and G. W. Yang, Appl. Phys. Lett. **95**, 232901 (2009).
[20] J. W. Hong, G. Catalan, D. N. Fang, E. Artacho, and J. F. Scott, arXiv:0908.3617 (unpublished).
[21] D. Yadlovker and Sh. Berger. Phys. Rev. B **71**, 184112 (2005).
[22] D. Yadlovker and Sh. Berger, Appl. Phys. Lett. **91**, 173104 (2007).
[23] D. Yadlovker and Sh. Berger, J. Appl. Phys. **101**, 034304 (2007).
[24] C.-G. Duan, S. S. Jaswal, and E. Y. Tsymbal, Phys. Rev. Lett. **97**, 047201 (2006).
[25] C. L. Wang and S. R. P. Smith, J. Phys.: Condens. Matter **7**, 7163 (1995).
[26] A. Sundaresan, R. Bhargavi, N. Rangarajan, U. Siddesh, and C. N. R. Rao, Phys. Rev. B **74**, 161306(R) (2006).
[27] E. Erdem, H.-Ch. Semmelhack, R. Bottcher, H. Rumpf, J. Banys, A. Matthes, H.-J. Glasel, D. Hirsch, and E. Hartmann, J. Phys.: Condens. Matter **18**, 3861 (2006).
[28] Z.-G. Ban, S. P. Alpay, and J. V. Mantese, Phys. Rev. B **67**, 184104 (2003).
[29] O. Madelung, *Semiconductors: Data Handbook*, 3rd ed. (Springer-Verlag, Berlin, 2004).
[30] A. N. Morozovska, E. A. Eliseev, R. Blinc, and M. D. Glinchuk, arXiv:0910.2421 (unpublished).
[31] S. Mukherjee, C. H. Chen, C. C. Chou, B. K. Chaudhuri, and H.-D. Yang, American Physical Society (unpublished).